

A New InP/InGaAs Double Heterojunction Bipolar Transistor (DHBT) With a Step-Graded InAlGaAs Collector Structure

Tzu-Pin Chen, Shiou-Ying Cheng¹, Ching-Wen Hung, Kuei-Yi Chu, Li-Yang Chen, Tsung-Han Tsai, and Wen-Chau Liu*

Institute of Microelectronics, College of Electrical Engineering and Computer Science, National Cheng Kung University

¹Department of Electrical Engineering, National Ilan University

Email: wcliu@mail.ncku.edu.tw

IEEE Electron Device Letters, Vol. 29, No. 1, pp. 11-14, Jan 2008.

Over the past years, InGaAs-based heterojunction bipolar transistors (HBTs) have attracted significant interest for microwave and low-power digital applications due to excellent transport properties of the InGaAs material. However, the intrinsic disadvantage of low breakdown voltage and high output conductance limit their applications in low-voltage and low-power dissipation digital circuits. On the other hand, double heterojunction bipolar transistors (DHBTs) have been used to improve the breakdown characteristics. Nevertheless, for DHBTs, an abrupt heterojunction at the B-C interface induces a large degradation of device performance caused by the current blocking effect. To overcome this problem, several approaches have been reported, such as p-n pair, composite collector structure, and a compositionally graded layer at the base-collector (B-C) junction to form the improved double heterojunction structures.



In this work, an interesting InP/InGaAs HBT with a step-graded InAlGaAs collector structure is presented and studied. The step-graded collector uses a quaternary InAlGaAs material between base and collector layer. In addition, the potential spike between base and collector layer can be effectively reduced due to the presence of this inserted quaternary InAlGaAs material. The quaternary InAlGaAs step-graded collector structure is composed of several graded layers with different energy band gaps. This variable band lineup is increased from base to collector layer. Due to the effectively larger bandgap of the composite collector structure, a larger collector breakdown electric field (voltage) can be expected.

The simulated energy band diagrams near the B-C junction of the conventional DHBT and the studied device at thermal equilibrium are shown in Fig. 1. The distribution of the base-collector barrier in the depleted collector region makes it possible for electrons with sufficient kinetic energy to transport over the conduction band spikes even at zero bias. The presence of the InGaAs setback layer near to the P⁺ InGaAs base is beneficial in minimizing the carrier blocking effect. Basically, this layer suspends the extension of the first conduction band spike into the base-collector space charge region, which can substantially block electrons transiting into the collector. Furthermore, the originally high and wide spike presented at the base/collector interface can be separated into some low and narrow spikes when the step-graded InAlGaAs layers are inserted between base-collector heterointerface. Therefore, the

improvement of collection efficiency of electrons can be obtained.

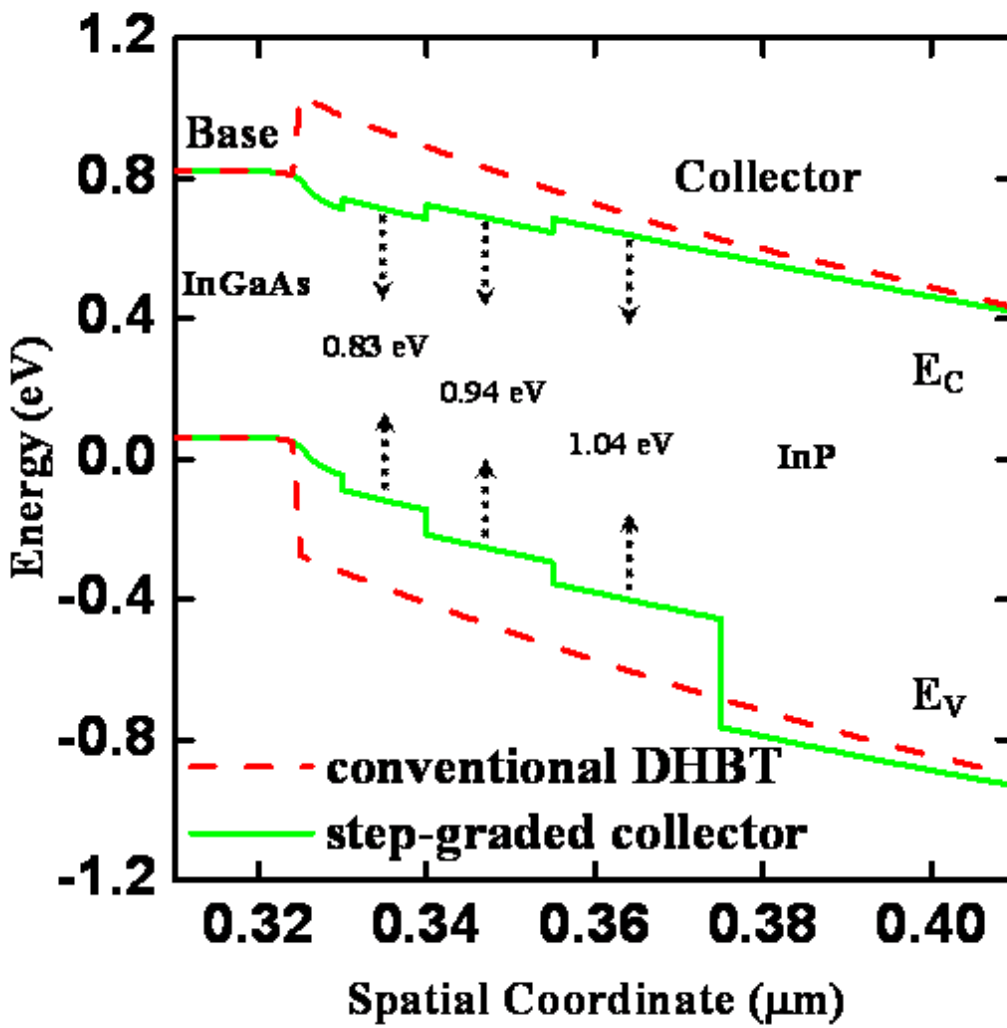


Fig. 1 The energy band diagram near the B/C junction of the conventional DHBT and the studied step-graded collector structure at thermal equilibrium.

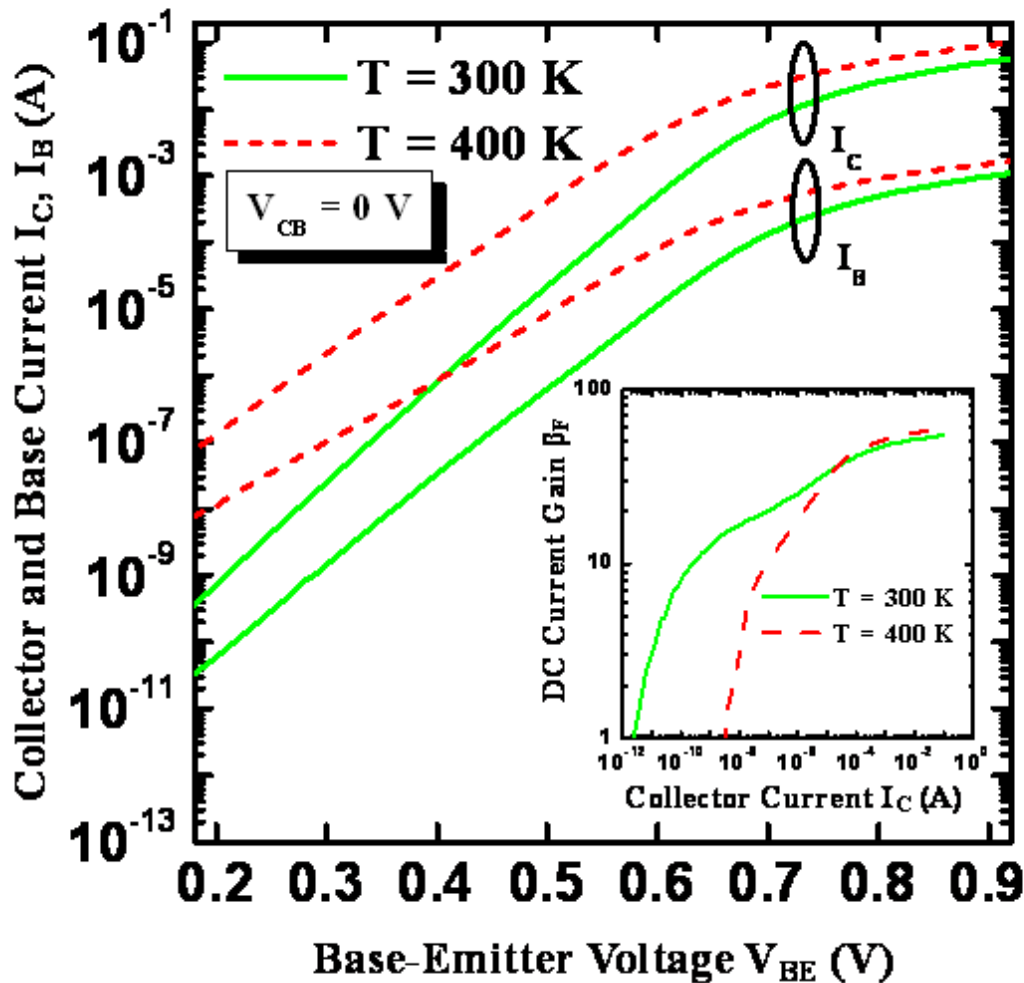


Fig. 2 The Gummel plots of the studied device at 300 and 400 K. The dependences of DC current gain β_F on the collector current I_C at 300 and 400 K are shown in the inset.

Figure 2 shows the Gummel plots of the studied DHBT measured at 300 and 400 K. The collector-base voltage is kept at $V_{CB} = 0$ V. The ideality factors of collector (base) current are 1.15 (1.27) and 1.1 (1.22) at 300 and 400 K, respectively. The ideality factor is primarily discussed by carrier transport on the conduction band at emitter/base (base/collector) junction. The 1-kT like collector current I_C indicates that the transport of conducting carrier is primarily dominated by the thermionic emission and diffusion mechanisms. The slightly deviation of n_C value from unity is mainly attributed to the tunneling current through the B-E (B-C) heterojunction. In addition, the decrease of n_C with elevating the temperature indicates the substantial importance of thermionic emission at higher temperature. The near unity of n_B value reveals that the bulk recombination current dominates the whole base current especially at higher temperature. Clearly, this good performance of ideality factors is directly related to the use of step-graded collector heterostructure. Furthermore, the studied device exhibits the low offset and saturation voltage of 98.4 mV and 0.33 V. Furthermore, the dependences of dc current gain β_F on the collector current I_C at 300 and 400 K are shown in the inset of Fig. 2. The collector-base voltage is fixed at $V_{CB} = 0$ V. The studied device can be operated under extremely wide collector current regimes. The operation regime is wider than 11 decades in magnitude of collector current ($I_C = 10^{-12}$ A to $I_C = 10^{-1}$ A). Experimentally, the current gain β_F of the studied device is greater than unity even at an extremely low

collector current of $I_c = 2.3 \times 10^{-12}$ A at 300 K. The observation of β_f at the extremely low current region is mainly caused by the insertion of the step-graded InAlGaAs collector structure. This step-graded InAlGaAs collector structure effectively reduces the potential spike at B-C heterointerface. Moreover, the higher dc current gain at 400 K is found as the collector current is increased to $I_c = 10^{-4}$ A. It is attributed to the high thermal collector leakage current with increasing the temperature. This gives a great contribution to the collector current I_C and results in higher dc current gains.

Figure 3 illustrates the typical common-emitter I-V characteristics of the studied device at 300 and 400K. Obviously, the device shows high common-emitter breakdown and low output conductance. As the temperature is increased, carriers within the collector region obtain more thermal energy and thus increase the probability of impact ionization. Hence, the contribution of thermal generation apparently plays a key role in the increase of collector current I_C . Experimentally, the common-emitter breakdown voltage of our studied device with the collector thickness of 400 nm, at $I_c = 100 \mu\text{A}$, is 8.05 V. Moreover, our studied device has a lower offset and saturation voltage, which certainly leads to a larger voltage operation range. When the temperature is elevated, the raised collector current arising from the positive temperature dependence of impact ionization coefficient in the collector causes the lower breakdown voltage. Moreover, the studied device shows nearly identical amplification even at the temperature up to 400K. These superior characteristics again indicate the potentiality of the studied device in practical circuit applications.

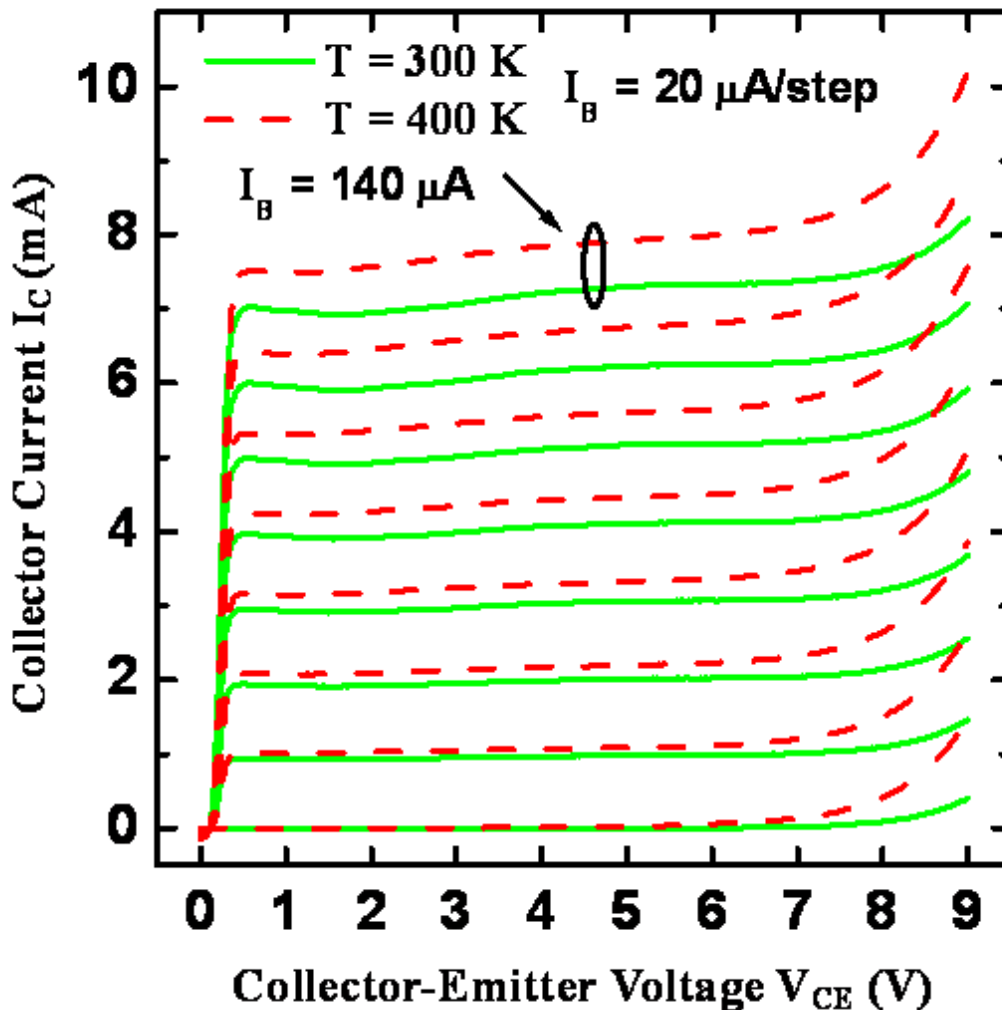


Fig. 3 Common-emitter current-voltage characteristics of the studied device at 300 and 400 K.

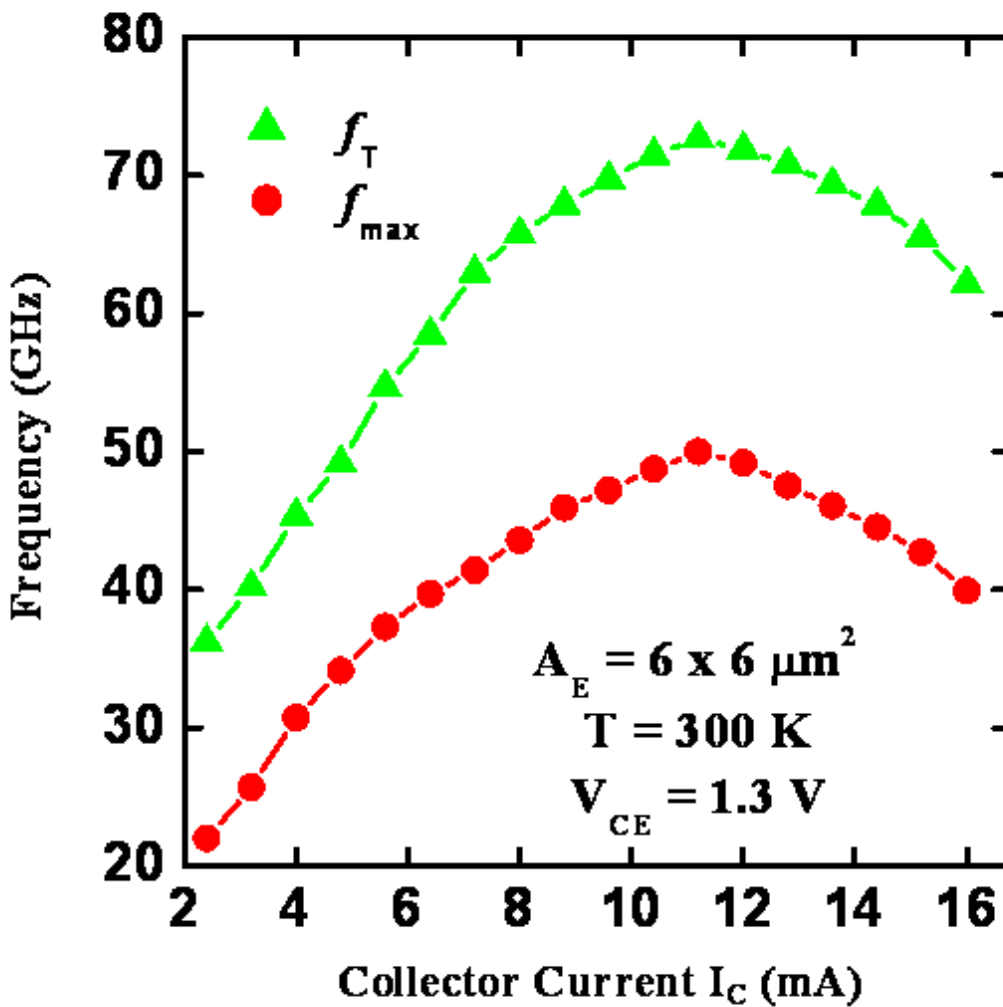


Fig. 4 Unity current gain cut-off frequency f_T and maximum oscillation frequency f_{max} versus collector current I_C for the studied device.

Figure 4 shows the dependences of unity current gain cut-off frequency f_T and maximum oscillation frequency f_{max} as a function of collector current I_C . For a nonoptimized device ($A_E = 6 \times 6 \mu\text{m}^2$), the peak f_T (f_{max}) of the studied device is 72.7 GHz (50 GHz). Clearly, due to the employment of the step-graded collector structure, the studied device exhibits excellent microwave characteristics. The fall-off phenomena of f_T and f_{max} at high collector current regions are caused by the Kirk effect and series resistance effect.

In conclusion, the dc and microwave characteristics of an interesting InP/InGaAs DHBT with a step-graded InAlGaAs collector structure are studied and demonstrated. Based on the employment of the step-graded InAlGaAs collector structure at the B-C heterojunction, the undesired electron blocking effect can be eliminated. Experimentally, the operation regime is wider than 11 decades in magnitude of collector current ($I_C = 10^{-12}$ A to $I_C = 10^{-1}$ A). Furthermore, the studied device shows a relatively high common-emitter breakdown voltage and low output conductance though at high temperature. Good

values of f_T (72.7 GHz) and f_{max} (50 GHz) have been obtained for a nonoptimized device.

References

- [1] J. Y. Chen, D. F. Guo, S. Y. Cheng, K. M. Lee, C. Y. Chen, H. M. Chuang, S. Y. Fu, and W. C. Liu, "A new InP–InGaAs HBT with a superlattice collector structure," *IEEE Electron Device Lett.*, vol. 25, no. 5, pp. 244–246, May 2004.
- [2] W. K. Huang, S. C. Huang, H. W. Chung, Y. M. Hsin, J. W. Shi, Y. C. Kao, and J. M. Kuo, "37-GHz bandwidth monolithically integrated InP HBT/evanescently coupled photodiode," *IEEE Photon. Technol. Lett.*, vol. 18, no. 12, pp. 1323–1325, Jun. 2006.
- [3] J. H. Tsai and Y. C. Kang, "DC performance of InP/InGaAs p-n-p heterostructure-emitter bipolar transistor," *IEEE Trans. Electron Devices*, vol. 53, no. 5, pp. 1265–1268, May 2006.
- [4] N. Parthasarathy, Z. Griffith, C. Kadow, U. Singiseti, M. J. W. Rodwell, X. M. Fang, D. Loubychev, Y. Wu, J. M. Fastenau, and A. W. K. Liu, "Collector–pedestal InGaAs/InP DHBTs fabricated in a single-growth, triple-implant process," *IEEE Electron Device Lett.*, vol. 27, no. 5, pp. 313–316, May 2006.
- [5] A. Feyngenson, D. Ritter, R. A. Hamm, P. R. Smith, P. K. Montgomery, R. D. Yadvish, H. Temkin, and M. B. Panish, "InGaAs/InP composite collector heterostructure bipolar transistors," *Electron. Lett.*, vol. 28, no. 7, pp. 607–609, Mar. 1992.

Copyright 2009 National Cheng Kung University